Published in final edited form as:
Biochemistry. 2011 May 31; 50(21): 4590–4596. doi:10.1021/bi2004069.

Thermodynamic compensation upon binding to exosite 1 and the active site of thrombin

Nicholas A. Treuheit, **Muneera A. Beach**, and **Elizabeth A. Komives***
Department of Chemistry and Biochemistry, University of California, San Diego La Jolla, CA 92093-0378

Abstract

Several lines of experimental evidence including amide exchange and NMR suggest that ligands binding to thrombin cause reduced backbone dynamics. Binding of the covalent inhibitor D-Phe-Pro-Arg chloromethylketone to the active site serine, as well as non-covalent binding of a fragment of the regulatory protein, thrombomodulin, to exosite 1 on the back side of the thrombin molecule both cause reduced dynamics. However, the reduced dynamics do not appear to be accompanied by significant conformational changes. In addition, binding of ligands to the active site does not change the affinity of thrombomodulin fragments binding to exosite 1, however, the thermodynamic coupling between exosite 1 and the active site has not been fully explored. We present isothermal titration calorimetry experiments that probe changes in enthalpy and entropy upon formation of binary ligand complexes. The approach relies on stringent thrombin preparation methods and on the use of dansyl-L-arginine-(3-methyl-1,5-pantanediyl) amide and a DNA aptamer as ligands with ideal thermodynamic signatures for binding to the active site and to exosite 1. Using this approach, the binding thermodynamic signatures of each ligand alone as well as the binding signatures of each ligand when the other binding site was occupied were measured. Different exosite 1 ligands with widely varied thermodynamic signatures cause the same reduction in ΔH and a concomitantly lower entropy cost upon DAPA binding at the active site. The results suggest a general phenomenon of enthalpy-entropy compensation consistent with reduction of dynamics/increased folding of thrombin upon ligand binding to either the active site or to exosite 1.

Keywords

Thrombin; thrombomodulin; serine protease; DNA aptamer; anticoagulant pathway; binding thermodynamics; anion-binding exosite

Thrombin is a dual-action protease that serves a pivotal function in the coagulation cascade where it participates in cleavage of fibrinogen to form blood clots but it also activates protein C initiating anticoagulation. Fibrinogen binds at two sites on thrombin, the active site where cleavage occurs, and exosite 1, on the opposite side of the thrombin molecule (Figure 1A). Thrombomodulin (TM) binds thrombin at exosite 1, (*1*, *2*), inhibits fibrinogen binding, and increases the catalytic activity toward protein C (cofactor activity) (*3*). The fourth, fifth, and sixth EGF-like domains of TM are all that is required for cofactor activity (*4*, *5*). The residues responsible for binding to thrombin are contained in the fifth and sixth

*Author to whom correspondence should be addressed: Department of Chemistry and Biochemistry U. C. San Diego La Jolla, CA 92093-0378 ph: (858) 534-3058 FAX: (858) 534-6174 ekomives@ucsd.edu.

Supplemental Information
Additional materials and data. This material is available free of charge via the Internet at http://pubs.acs.org

domains, and residues in the fourth domain are necessary for protein C activation (*6-8*)}. Two EGF-like domain-containing fragments of TM that have been employed to study TM-thrombin interactions include TMEGF45, which has full cofactor activity, but binds 10-fold more weakly, and TMEGF56, which does not have cofactor activity, but has full binding affinity (*7*).

TM binding to thrombin at exosite 1 has been shown to greatly increase the binding rate of various inhibitors that bind at the active site of thrombin (*2, 9-12*) and the k_a for protein C binding has been shown to be 1000-fold higher for the TM-thrombin complex compared to thrombin alone (*13*). However, TM binding did not measurably alter the structure of thrombin (*14*) possibly due to the presence of an irreversible inhibitor, L-Gly-Gly-Arg chloromethyl ketone (GGACK), which is very similar to $_D$Phe-Pro-Arg-chloromethyl ketone (PPACK), in the active site of thrombin which dramatically decreases the dynamics of the complex (*15*). In addition, different changes in the spectra of fluorescent dyes bound to the active site of thrombin were observed depending on whether cofactor-active or inactive fragments of TM were bound at exosite 1 (*16*). More recently, H/D exchange experiments have been used to probe changes in the backbone dynamics of thrombin when bound to TMEGF45 and TMEGF56 (*17*). Two regions, one that was part of a β-strand connecting exosite 1 to the active site (residues Leu84 to Leu99 using the chymotrypsin numbering scheme), retained more deuterium when bound to TMEGF45 compared to TMEGF56. Figure 1A highlights exosite 1 and the active site of thrombin as well the β-strand that connects them. Although all of these results suggest an allosteric linkage between exosite 1 and the active site, thermodynamic coupling between these two binding sites has not been measured directly by calorimetry.

Thermodynamic measurements give powerful insights for understanding the interactions of receptors and their ligands, and isothermal titration calorimetry (ITC) is a tool that can be used to directly measure all the thermodynamic properties of a binding event. Interactions between a monoclonal antibody and thrombin, as well as between TM and thrombin have been examined previously by ITC, but the TM-thrombin interaction appears to be entirely entropic and so it could not be studied further with this method (*18*). Recently, ITC was used to examine the binding of ligands to the thrombin active site and to exosite 2 (*19*). Here, we have probed the thermodynamic coupling between exosite 1 and the active site using ITC.

In order to further investigate the effects of various ligands binding to thrombin, we used a methyl analog of dansyl-L-arginine-(3-ethyl-1,5-pantanediyl) amide (DAPA) (*20*) called DAMPA, that was previously used to study pH effects upon binding to thrombin (*21*) as a reversible active site ligand. The thrombin-binding DNA aptamer was used as a reversible ligand that binds at exosite 1 (*22*). Both DAMPA and the DNA aptamer bind with high affinity and a significant change in enthalpy. The effects of different ligands binding alone and in combination reveal thermodynamic coupling between exosite 1 and the active site. Binding at the active site changes the thermodynamic signature of exosite 1 ligands and conversely binding at exosite 1 changes the thermodynamic signature of active site ligands.

Materials and Methods

Preparation of thrombin

Bovine thrombin was purified from a barium citrate eluate (prepared from bovine plasma) according to previously published methods (*23*). The eluate powder (5g) was redissolved overnight in 200 mL of 100 mM EDTA, 10 mM sodium citrate, and 150 mM NaCl containing 11.1g of ammonium sulfate and 30mg of benzamidine. Following resuspension, the concentration of ammonium sulfate was increased from 10 to 40%. After centrifugation at 10,000g for 20 min, the supernatant was kept, brought to 70% ammonium sulfate, and

centrifuged. The pellet, containing prothrombin, was dissolved in 5 mL of 50 mM Tris (pH 7.5) and 150 mM NaCl and loaded onto a G-25 Sephadex gel filtration column (2.5 cm × 100 cm) to remove the ammonium sulfate, and the fraction containing the protein was collected. The prothrombin was activated by incubating it with 2.0 mg/mL *Echis carinatus* venom (Miami Serpentarium), 10 mM $CaCl_2$, and 1 mg/mL PEG-8000 for 45 min at 37°C. The mixture was loaded onto a second G-25 Sephadex (2.5 cm × 100 cm) equilibrated in 25 mM KH_2PO_4 (pH 6.5) and 100 mM NaCl, and the protein fraction was collected. Finally, the G-25 fraction containing active thrombin was loaded onto a MonoS FPLC 16/10 column (Amersham/GE Healthcare) equilibrated with buffer A [25 mM KH_2PO_4 (pH 6.5) and 100 mM NaCl]. The thrombin was eluted with a linear gradient of buffer B [25 mM KH_2PO_4 (pH 6.5) and 500 mM NaCl] over the course of 90 minutes. Purified, active α-thrombin was identified by fibrinogen clotting. Active fractions (>4000 U/mg) were stored in 1 mL aliquots with 10 mM benzamidine at -80°C for up to two weeks. For PPACK thrombin, 1 mL fractions of active α-thrombin were added to 1.1 μmol lyphoilized aliquots of PPACK and allowed to shake for 3 hours at room temperature before storing at -80°C. Immediately before ITC, all proteins were re-purified by HiLoad 16/60 Superdex 75 size-exclusion chromatography (Amersham/GE Healthcare) equilibrated in 50 mM Bis-tris propane (pH 7.4), 150 mM NaCl, (and 2.5 mM $CaCl_2$ for the experiments in calcium-containing buffer). This step removes the benzamidine, after which time the thrombin was used within 8 hrs.

Preparation of TMEGF45

TMEGF45 was expressed in *Pichia pastoris* yeast as described previously (*7*). The protein was first purified by anion-exchange chromatography (QAE Sephadex followed by HiLoad 26/10 Q Sepharose) followed by reverse-phase HPLC as described previously (*24*). HPLC fractions with specific activities above 3×10^4 nmol apC/min/mg TM were lyophilized and stored at -20°C. The lyophilized fractions were finally reconstituted in DI H_2O and purified by HiLoad 16/60 Superdex 75 size-exclusion chromatography (Amersham/GE Healthcare) in 50 mM Bistris propane (pH 7.4), 150 mM NaCl.

Preparation of DAMPA

Due to the lack of availability of 4-ethylpiperidine, required for the synthesis of DAPA as described in (*20*), we modified the procedure to use 4-methylpiperidine, which is readily available, instead. This procedure results in DAMPA, which was also previously described, but by a simpler synthetic approach (*21*). Dansyl arginine HCl (75 mg, 0.169 mmol) and N,N-carbonyldiimidazole (180 mg, 1.11 mmol) were added to 600 μL of DMSO and allowed to stir for 2 min. Then 180 μL of 4-methylpiperidine was added and the reaction was allowed to stir for 4 hours at room temperature in the dark. The reaction was quenched with 2 mL of 150 mM NaCl and extracted twice with ethyl acetate. The ethyl acetate layer containing the crude DAMPA was evaporated over the course of an hour with a directed stream of N_2, leaving a yellow oil which was resuspended in warm 0.1% TFA, 15% acetonitrile (ACN) and immediately injected on a Waters C18 reverse phase column (19 mm × 300 mm) equilibrated with 0.1% TFA/10% ACN. DAMPA was eluted by a gradient of 0-50% ACN over 30 minutes at a flow rate of 10 mL/min. Fractions were collected and analyzed by MALDI-MS; DAMPA has a molecular weight of 489.3 g/mol. Fractions containing only DAMPA were lyophilized out of H_2O and stored at -80°C for up to 3 months in 4.2 nmol aliquots. The concentration of DAMPA was determined by the absorbance at 330 nm ($\varepsilon = 4010$ cm L unit^{-1} mol^{-1}).

DNA Aptamer

The 15 base DNA aptamer, GGTTGGTGTGGTTGG, originally discovered by Bock et al., from a screen of 10^{13} synthetic oligonucleotides (*22*), binds thrombin at exosite 1, and was ordered from Integrated DNA Technologies. Samples were lyophilized in 43 nmol aliquots

and stored at -20°C until needed. Immediately before use, the samples were reconstituted in 600 μL of ITC buffer. Concentration was determined by the absorbance at 260 nm (ε = 143300 cm L unit^{-1} mol^{-1}).

ITC Experiments

All proteins were re-purified by size-exclusion chromatography the same day the experiments were performed (see above). Protein concentrations were determined by BCA assay (Pierce Chemicals). Collected fractions were concentrated to 6.5 μM and stored at -20°C for the day until they were used. DAMPA and thrombin aptamer samples were reconstituted in 50 mM Bis-tris propane (pH 7.4), 150 mM NaCl, (and 2.5 mM $CaCl_2$ for the experiments in calcium-containing buffer) to final concentrations of 65-70 μM. For TMEGF45-thrombin experiments, 13 nmol of re-purified thrombin were combined with 65 nmol of re-purified TMEGF45 and concentrated to a final volume of 2 mL, yielding a final concentration of 6.5 μM thrombin and a 5-fold excess of TMEGF45, ensuring that the thrombin was >99% bound with the TMEGF45 (*25*).

All ITC experiments were performed on a VP-ITC calorimeter (MicroCal, Inc). The volume of the calorimetric cell in the VP-ITC is 1.4 mL and all titrations detailed in this paper were conducted by adding the titrant in steps of 10 μL. All experiments were performed at 25°C with a 180 second initial delay. In order to avoid bubble formation in the calorimetric cell during stirring, all solutions were thoroughly degassed. The heat evolved during each injection of ligand was obtained by integrating the calorimetric signal. The heat associated with binding of a ligand to the protein in the cell was obtained by subtracting the heat of dilution from the heat of reaction. Heats of dilution due to mismatch between the syringe and cell solutions were insignificant in all experiments. The individual heats were plotted as a function of the molar ratio, and nonlinear regression of the data was performed using the ORIGIN software supplied with the instrument according to a single binding site model, which provided the enthalpy change (ΔH) and the binding constant (K_A).

Differential Scanning Calorimetry (DSC) Experiments

Immediately before DSC, all proteins were re-purified by HiLoad 16/60 Superdex 75 size-exclusion chromatography (Amersham/GE Healthcare) equilibrated in 25 mM PIPES pH 6.5, and 150 mM NaCl. Samples containing 25 μM thrombin, 75 μM TMEGF45, 50 μM DAMPA or 50 μM aptamer were degassed for 10 minutes prior to DSC analysis. All melting experiments were performed on a VP-DSC calorimeter from MicroCal Inc with an active cell volume of 0.5 mL. Melting experiments were performed over a range of 25-90°C with a scan rate of 90°C/hour and sets of experiments were always preceded by an initial buffer scan followed by dynamic loading of samples during a thermal downscan.

Results

Binding of ligands to the active site and to exosite 1 of thrombin

With the goal of probing how ligand binding at exosite 1 might affect the thermodynamics of binding at the active site, we tested various ligands that were known to bind at each of these sites. The fluorescent ligand, DAPA, which has often been used for active site titration (*20*), has exothermic binding with a ΔH of -6 kcal/mol and an equilibrium binding dissociation constant of 22 nM. Due to uneven quality of commercially-available DAPA, an analog, DAMPA was synthesized that gave an essentially identical thermodynamic signature (Figure 1B, Table 1). Experiments were all performed at 25°C in order to minimize autocatalytic degradation of thrombin. SDS-PAGE analysis of the thrombin re-obtained from the ITC cell after an experiment in which DAMPA binding was measured showed that the thrombin had not been significantly autolyzed (Supplementary Figure 1). Thus, the

binding of DAMPA gives a convenient thermodynamic signature of binding to the active site of thrombin that is indistinguishable from the binding of DAPA (*19*).

We previously showed that TMEGF45 shows no change of heat when it binds to thrombin, thus making it a poor choice of ligand for probing binding to exosite 1 (*18*). Here we show that TMEGF56, which binds 10-fold more strongly to thrombin than TMEGF45, also does not release heat upon binding to thrombin (Figure 1C). This same preparation of TMEGF56 bound tightly to thrombin with a K_D of 1.7 nM as assessed by SPR (Supplemental Figure 2) (*26*). Thus, it appears that fragments of TM do not provide a directly measurable thermodynamic signature of binding to exosite 1. In contrast, a DNA aptamer selected to bind to exosite 1 was highly exothermic with a ΔH of -20.2 kcal/mol and an equilibrium binding dissociation constant of 111 nM (Figure 1D, Table 1). The results were indistinguishable whether human or bovine thrombin was used (Supplementary Figure 3), so experiments were performed with bovine thrombin for cost efficiency. The results show that different exosite 1 ligands have markedly different thermodynamic signatures.

Binding of the DNA aptamer to exosite 1 alters the thermodynamics of binding at the active site

The binding of single ligands to either the active site or exosite 1 gave clear thermodynamic signatures that could be reproducibly measured by ITC. We next used these same ligands to probe the thermodynamic cross-talk between exosite1 and the active site. In these experiments, a complex was pre-formed between thrombin and one of the ligands and then this complex was titrated in the ITC with the other ligand. The amount of the first ligand added to form the complex was determined from the ITC titrations shown in Figure 1 and a sufficient excess was added so that the thrombin was completely bound. We first probed the effects of binding the DNA aptamer to exosite 1 prior to titrating the active site with DAMPA. The results showed that when the DNA aptamer was bound, the heat released (ΔH) upon binding DAMPA was significantly reduced from -5.9 kcal/mol upon binding DAMPA to free thrombin to only to only -4.2 kcal/mol upon binding DAMPA to the aptamer-thrombin complex (Figure 2). Remarkably, the binding affinity was nearly the same with a ΔG of -10.4 kcal/mol for DAMPA binding to free thrombin *vs*. a ΔG of -10.5 for DAMPA binding to the aptamer-thrombin complex (Table 1). The reason for the large difference in heat released compared to the small difference in ΔG between the two binding reactions is accounted for by a compensating difference in the entropy change upon binding. We report the entropy change as –TΔS so that it can be directly compared to the ΔH and ΔG. For DAMPA binding to thrombin, the -TΔS was -4.4 kcal/mol whereas the –TΔS was -6.4 kcal/mol for DAMPA binding to the aptamer-thrombin complex (Table 1). Use of DAMPA as the ligand in these experiments was convenient because its K_A is in a good range of c values so that the stoichiometry and K_A could be reliably obtained directly from the ITC experiment. The value of ΔG was then obtained from the ITC measurement of K_A, and finally the value of -TΔS was computed from ΔG-ΔH.

Binding of the DNA aptamer to free thrombin has a different thermodynamic signature from binding of the DNA aptamer to PPACK-thrombin

To ascertain whether the alteration in thermodynamic signature “goes both ways” in thrombin, we next compared the thermodynamics of binding of the DNA aptamer to free thrombin *vs*. PPACK-thrombin. Again, the heat released upon binding of the DNA aptamer to PPACK-thrombin was significantly less than for binding of the DNA aptamer to free thrombin (Figure 3). In this case, the overall ΔG for these two binding events was very similar (-9.7 *vs*. -9.4 kcal/mol) and the difference in the entropy change upon binding again compensated for the difference in heat released (Table 1).

Effect of TMEGF45 on the thermodynamics of DAMPA binding to thrombin

To test whether TM binding also affects ligand binding at the active site, binding of DAMPA to free thrombin was compared to binding of DAMPA to the thrombin-TMEGF45 complex. As with the aptamer, the ΔH upon DAMPA binding to free thrombin was significantly more favorable than the ΔH upon DAMPA binding to the thrombin-TMEGF45 complex (Figure 4). The enthalpy change upon binding was reduced from -5.9 kcal/mol to -4.5 kcal/mol and the entropy change again fully compensated for the difference so that the difference in binding free energy between the two experiments was negligible (Table 1). This result was all the more remarkable considering the completely different thermodynamic signature of the aptamer binding (highly favorable ΔH) compared to TMEGF45 binding (no observable binding ΔH).

Effects of calcium on the binding thermodynamics of ligand binding

Although thrombin is not thought to have a calcium-binding site, experiments on TM binding to thrombin are usually carried out in buffer containing calcium because both TM and protein C are known to bind calcium (*27*, *28*). We thus repeated all of the experiments already described in buffer containing 2.5 mM $CaCl_2$ (Table 1). The thermodynamic signature of DAMPA binding to thrombin was within error the same whether the buffer contained calcium or not (Table 1). Consistent with the ionic nature of the interaction between the DNA aptamer and exosite 1 of thrombin, the thermodynamic signature for the aptamer binding changed slightly so that the binding ΔH was slightly more favorable and the -TΔS was slightly less favorable. These differences were only slightly outside of the experimental error, and were judged to be insignificant. We also compared the differences between each thermodynamic parameter measured in the presence and absence of calcium for the ternary interactions (Figure 5). These results showed again that the enthalpy-entropy compensation is nearly complete also in the presence of calcium. In all cases, the same trends were observed for the ternary interactions in the presence or absence of calcium. For example, pre-binding of the DNA aptamer caused the ΔH to be somewhat more favorable and the –TΔS to be somewhat less favorable for DAMPA binding, and this trend was also seen in the presence of calcium (Figure 5A). Pre-binding of TMEGF45 also showed similar trends (Figure 5B). Attempts to measure a change in heat upon addition of calcium to thrombin in the cell showed no measurable direct binding indicating that the calcium effects are most likely secondary ionic effects most likely influencing binding at exosite 1.

Relationship between binding and overall thrombin stabilization

One explanation for the decreased entropic penalty for binding a ligand at one site when a ligand is already bound at another site is that the first ligand reduces the dynamics of the protein so that a smaller conformational entropy change occurs upon binding the second ligand (*29*). We previously showed that when PPACK is bound at the active site of thrombin the backbone dynamics are reduced throughout the protein (*15*). The reduced dynamics are accompanied by a large increase in stabilization; the T_m increases from 57°C to 70°C as measured by DSC (*30*). To probe whether something similar happens when ligands bind to exosite 1, we performed DSC experiments to compare the stability of thrombin alone to thrombin bound with the aptamer or TMEGF45 at exosite 1. Both the aptamer and TMEGF45 caused a small but measureable increase in melting temperature (57.9°C) as compared to thrombin alone (56.9°C) (Figure 6A) however the change was much smaller than that observed for PPACK binding to the active site (*30*). Thus, the thermodynamic coupling between exosite 1 and the active site may be partially, but not completely attributed to alterations of conformational dynamics.

Discussion

Direct thermodynamic measurement of binding allostery in thrombin has been a difficult goal to achieve for several reasons. First, the concentration of thrombin required for ITC measurements is relatively high, and under these conditions, thrombin autolysis is expected to be significant. We circumvented this problem by using freshly-prepared thrombin that was stored briefly at -80°C at pH 6.5 with 5mM benzamidine, then re-purified by size exclusion chromatography and rapidly concentrated immediately before the ITC experiment was performed. These measures ensured that all of the thrombin was fully binding competent allowing accurate measurement of the stoichiometry and heat released upon binding.

As reviewed in the introduction, previous work by us and others, particularly focused on the binding of TM fragments to exosite 1, suggested that binding at exosite 1 somehow changes the active site of thrombin (*16, 17*). Although these results hinted that the binding sites may engage in “allosteric communication”, binding affinities (K_D) measured by SPR were exactly the same for active thrombin binding to TMEGF456 vs. PPACK-inactivated thrombin binding to TMEGF456 (*18, 31*). As allostery is traditionally defined as a change in ΔG of binding at one site when the allosteric site is occupied, this result should be interpreted as the absence of allostery between exosite 1 and the active site.

The results we present here definitely demonstrate thermodynamic coupling between exosite 1 and the active site, however the coupling does not result in a change in ΔG as would be expected for traditional allostery. Instead what is observed is a near perfect enthalpy-entropy compensation. Two different ligands, a DNA aptamer and a TM fragment were used as ligands at exosite 1. Two different ligands, a covalent PPACK modification at Ser 195 and a non-covalent ligand, DAMPA, were used to probe binding at the active site. To look for allostery, we measured the difference in binding thermodynamics at the one site in the presence or absence of a ligand pre-bound at the other site. These experiments revealed, as expected, that the allosteric coupling “runs in both directions”. That is, if a ligand is bound at exosite 1, the binding ΔH at the active site is reduced, but also the entropic cost is lower so the overall binding ΔG doesn't change. Similarly, if a ligand was bound at the active site, the heat released upon binding a ligand at exosite 1 was reduced and the entropic cost lowered so that again the binding ΔG doesn't change.

Such an enthalpy-entropy compensation mechanism is most often seen in protein folding reactions where a the protein adopts a large number of conformations in the unfolded state (high entropy) and when the protein folds to a single native state this entropy is exchanged for the favorable enthalpy of specific side chain interactions in the folded structure. It is tantalizing to speculate that ligand binding to either site on thrombin in effect further folds the protein and that this is what we are observing in the binding experiments. It is well-known that thrombin is highly dynamic. Indeed, ligand binding to either exosite 1 or the active site reduced amide hydrogen exchange throughout thrombin (*15, 17*). Recent NMR experiments also showed that some resonances that were presumably exchange-broadened in free thrombin could be observed in the ligand-bound states again hinting at reduced dynamics upon ligand binding (*32*). One interpretation of both of these results is that ligand binding changes the energy landscape of thrombin towards a more folded structure. This interpretation is bolstered by the finding that thrombin is highly stabilized towards thermal denaturation by ligand binding as measured by DSC (*15*).

Probably the most fascinating part of the story, however, is that it doesn't seem to matter what the ligand is. The two ligands that bound to exosite 1 had completely different thermodynamic signatures; the DNA aptamer bound with a highly favorable ΔH and a

highly unfavorable -TΔS whereas the TMEGF45 showed no change in enthalpy upon binding and presumably bound with a favorable -TΔS. It is worth emphasizing that even though we did not directly observe a change in heat upon TMEGF45 binding, the large difference in binding enthalpy when DAMPA was bound to free thrombin *vs*. the TMEGF45-thrombin complex is clear evidence that the TMEGF45 was, in fact, bound. Despite the completely different thermodynamic signatures, and even the completely different bound structures (Figure 6B), both of these ligands induced the same effects on DAMPA binding. Both reduced the favorable binding ΔH and in both cases this was compensated by a reduced entropic cost so that the overall binding ΔG was the same. The fact that such different ligands could induce similar thermodynamic changes in the active site strongly argues that they both caused similar folding changes in thrombin. The results presented here are consistent with previous H/D exchange results from our laboratory showing that ligand binding at exosite 1 decreased the amide exchange at the active site. This was true for cofactor-active fragments of TM as well as cofactor-inactive fragments (*17*). The results presented here, however, do not help to explain why different ligands, specifically cofactor active vs. inactive forms of TM induced different H/D exchange effects in loops surrounding the active site. It is likely that kinetics and not thermodynamics studies will be required to completely understand the dynamics changes induced by cofactor-active forms of TM.

Supplementary Material

Refer to Web version on PubMed Central for supplementary material.

Acknowledgments

N.A.T. acknowledges support from the Cell and Molecular Genetics Training Program. This work was funded by NIH grant RO1-HL070999.

Financial support for this work was provided by NIH grant RO1-HL070999 to EAK.

ABBREVIATIONS

ITC	isothermal titration calorimetry
DSC	differential scanning calorimetry
DAPA	dansyl-L-arginine-(3-ethyl-1,5-pantanediyl) amide
DAMPA	dansyl-L-arginine-(3-methyl-1,5-pantanediyl) amide
TM	thrombomodulin
TFA	trifluoroacetic acid
ACN	acetonitrile

References

1. Ayala YM, Cantwell AM, Rose T, B. L. A, A. D, Di Cera E. Molecular Mapping of Thrombin-Receptor Interactions, Proteins: Struct, Funct. Genet. 2001; 45:107–116.
2. Myles T, Church F, Whinna H, Monard D, Stone SR. Role of thrombin anion-binding exosite-I in the formation of thrombin-serpin complexes. J Biol Chem. 1998; 273:31203–31208. [PubMed: 9813026]
3. Esmon CT. Regulation of blood coagulation. Biochimica et Biophysica Acta. 2000; 1477:349–360. [PubMed: 10708869]

4. Hayashi T, Zushi M, Yamamoto S, Suzuki K. Further localization of binding sites for thrombin and protein C in human thrombomodulin. J Biol Chem. 1990; 265:20156–20159. [PubMed: 2173698]
5. Stearns DJ, Kurosawa S, Esmon CT. Microthrombomodulin. Residues 310-486 from the epidermal growth factor precursor homology domain of thrombomodulin will accelerate protein C activation. J Biol Chem. 1989; 264:3352–3356. [PubMed: 2536746]
6. Kurosawa S, Stearns DJ, Jackson KW, Esmon CT. A 10-kDa cyanogen bromide fragment from the epidermal growth factor homology domain of rabbit thrombomodulin contains the primary thrombin binding site. J Biol Chem. 1988; 263:5993–5996. [PubMed: 2834358]
7. White CE, Hunter MJ, Meininger DP, White LR, Komives EA. Large-scale expression, purification and characterization of small fragments of thrombomodulin: the roles of the sixth domain and of methionine 388. Protein Eng. 1995; 8:1177–1187. [PubMed: 8819984]
8. Koeppe J, Beach M, Baerga-Ortiz A, Kerns J, Komives E. Mutations in the fourth EGF-like domain affect thrombomodulin-induced changes in the active site of thrombin. Biochemistry. 2008; 47:10933–10939. [PubMed: 18803401]
9. Rezaie AR, Cooper ST, Church FC, Esmon CT. Protein C inhibitor is a potent inhibitor of the thrombin-thrombomodulin complex. J Biol Chem. 1995; 270:25336–25339. [PubMed: 7592694]
10. Rezaie AR, He X, Esmon CT. Thrombomodulin increases the rate of thrombin inhibition by BPTI. Biochemistry. 1998; 37:693–699. [PubMed: 9425093]
11. De Cristofaro R, Landolfi R. Allosteric modulation of BPTI interaction with human alpha- and zeta-thrombin. Eur. J. Biochem. 1999; 260:97–102. [PubMed: 10091588]
12. van de Locht A, Bode W, Huber R, Le Bonniec BF, Stone SR, Esmon CT, Stubbs MT. The thrombin E192Q-BPTI complex reveals gross structural rearrangements: implications for the interaction with antithrombin and thrombomodulin. Embo Journal. 1997; 16:2977–2984. [PubMed: 9214615]
13. Xu H, Bush LA, Pineda AO, Caccia S, Di Cera E. Thrombomodulin changes the molecular surface of interaction and the rate of complex formation between thrombin and protein C. J Biol Chem. 2005; 280:7956–7961. [PubMed: 15582990]
14. Fuentes-Prior P, Iwanaga Y, Huber R, Pagila R, Rumennik G, Seto M, Morser J, Light DR, Bode W. Structural basis for the anticoagulant activity of the thrombin-thrombomodulin complex. Nature. 2000; 404:518–525. [PubMed: 10761923]
15. Koeppe J, Komives E. Amide H/2H exchange reveals a mechanism of thrombin activation. Biochemistry. 2006; 45:7724–7732. [PubMed: 16784223]
16. Ye J, Esmon NL, Esmon CT, Johnson AE. The active site of thrombin is altered upon binding to Thrombomodulin. J Biol Chem. 1991; 266:23016–23021. [PubMed: 1660464]
17. Koeppe JR, Seitova A, Mather T, Komives E. Thrombomodulin tightens the thrombin active site loops to promote protein C activation. Biochemistry. 2005; 44:14784–14791. [PubMed: 16274226]
18. Baerga-Ortiz A, Bergqvist SP, Mandell JG, Komives EA. Two different proteins that compete for binding to thrombin have opposite kinetic and thermodynamic profiles. Protein Sci. 2004; 13:166–176. [PubMed: 14691232]
19. Kamath P, Huntington JA, Krishnaswamy S. Ligand Binding Shuttles Thrombin along a Continuum of Zymogen- and Proteinase-like States. J Biol Chem. 2010; 285:28651–28658. [PubMed: 20639195]
20. Nesheim M, Prendergast F, Mann K. Interactions of a fluorescent active-site-directed inhibitor of thrombin: Dansylarginine N-(3-ethyl-1,5-pentanediyl)amide. Biochemistry. 1979; 18:8.
21. Stone SR, Betz A, Hofsteenge J. Mechanistic Studies on Thrombin Catalysis. Biochemistry. 1991; 30:9841–9848. [PubMed: 1911776]
22. Bock LC, Griffin LC, Latham JA, Vermaas EH, Toole JJ. Selection of single-stranded DNA molecules that bind and inhibit human thrombin. Nature. 1992; 355:564–566. [PubMed: 1741036]
23. Ni F, Konishi Y, Scheraga HA. Thrombin-bound conformation of the C-terminal fragments of hirudin determined by transferred nuclear Overhauser effects. Biochemistry. 1990; 29:4479–4489. [PubMed: 2350549]
24. Wood MJ, Komives EA. Production of large quantities of isotopically labeled protein in Pichia pastoris by fermentation. J Biomol NMR. 1999; 13:149–159. [PubMed: 10070756]

25. Mandell JG, Baerga-Ortiz A, Akashi S, Takio K, Komives EA. Solvent accessibility of the thrombin-thrombomodulin interface. J Mol Biol. 2001; 306:575–589. [PubMed: 11178915]
26. Beach, M. Ph. D Thesis. Department of Chemistry and Biochemistry; UC San Diego: 2009. Thermodynamics of the Thrombin-Thrombomodulin Interaction.
27. Light DR, Glaser CB, Betts M, Blasko E, Campbell E, Clarke JH, McCaman M, McLean K, Nagashima M, Parkinson JF, Rumennik G, Young T, Morser J. The interaction of thrombomodulin with Ca2+. Eur J Biochem. 1999; 262:522–533. [PubMed: 10336638]
28. Colpitts T, Prorok M, Castellino F. Binding of Calcium to Individual Gamma-Carboxyglutamic Acid Residues of Human Protein C. Biochemistry. 1995; 34:2424–2430. [PubMed: 7873521]
29. Tsai C, del Sol A, Nussinov R. Allostery: Absence of a Change in Shape Does Not Imply that Allostery is not at Play. J Mol Biol. 2008; 378:1–11. [PubMed: 18353365]
30. Croy CH, Koeppe JR, Bergqvist S, Komives EA. Allosteric Changes in Solvent Accessibility Observed in Thrombin upon Active Site Occupation. Biochemistry. 2004; 43:5246–5255. [PubMed: 15122890]
31. Baerga-Ortiz A, Rezaie AR, Komives EA. Electrostatic dependence of the thrombin-thrombomodulin interaction. J Mol Biol. 2000; 296:651–658. [PubMed: 10669614]
32. Lectenberg B, Johnson D, Freund S, Huntington J. NMR Resonance Assignments of Thrombin Reveal the Conformational and Dynamic Effects of Ligation. Proc Natl Acad Sci U S A. 2010; 107:14087–14092. [PubMed: 20660315]
33. Bode W, Mayr I, Baumann U, Huber R, Stone S, Hofsteenge J. The refined 1.9 A crystal structure of human alpha-thrombin: interaction with D-Phe-Pro-Arg chloromethyl ketone and significance or the Tyr-Pro-Pro-Trp insertion segment. Embo Journal. 1989; 8:3467–3475. [PubMed: 2583108]
34. Padmanabhan K, Parmanabhan K, Ferrara J, Sadler J, Tulinsky A. The structure of alpha-thrombin inhibited by a 15-mer single stranded DNA aptamer. J Biol Chem. 1993; 268:17651–17654. [PubMed: 8102368]

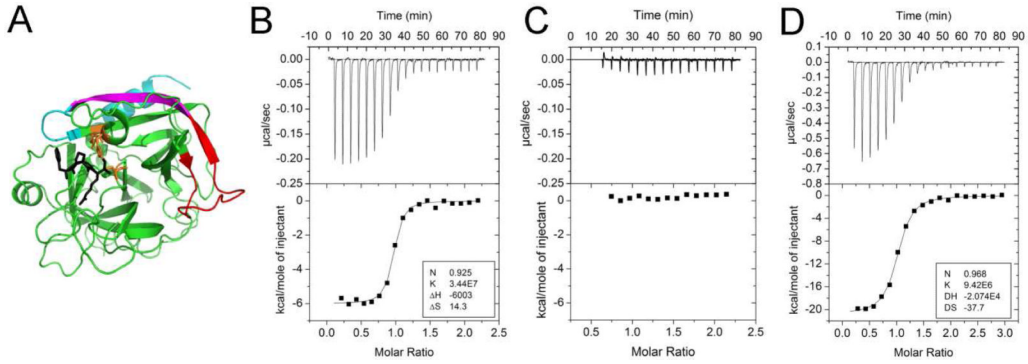

Figure 1.

(A) Crystal structure of PPACK thrombin (PDB 1PPB (*33*)). The catalytic triad is highlighted in orange, exosite 1 is shown in red, with the β-strand linking exosite 1 to the active site highlighted in purple, and the two peptides with reduced H/D exchange in the presence of TMEGF45 shown in cyan. The covalently bound PPACK is colored black. Representative ITC binding curves are shown for addition of 15 μL injections of a 70 μM solution of DAPA (B), or a 13 μM solution of TMEGF56 (C), or a 70 μM solution of the thrombin aptamer (D) to thrombin (6.5 μM in the cell). Values for K_a are M^{-1}, ΔH in $Jmol^{-1}$, ΔS in $Jmol^{-1*}K^{-1}$, and N is the stoichiometry of binding.

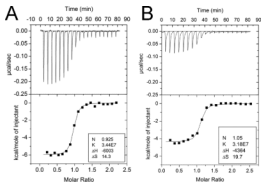

Figure 2.
ITC binding curves for the addition of 15 μL injections of a 70 μM DAPA solution binding to thrombin alone (6.5 μM in the cell) (A) and DAPA binding to a thrombin-aptamer complex (6.5 μM thrombin with 20 μM aptamer) (B).

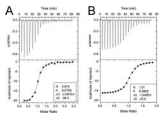

Figure 3.
ITC binding curves for 15 μL injections of a 70 μM aptamer solution binding to a 6.5 μM solution of thrombin (A) and to a 6.5 μM solution of PPACK-thrombin (B).

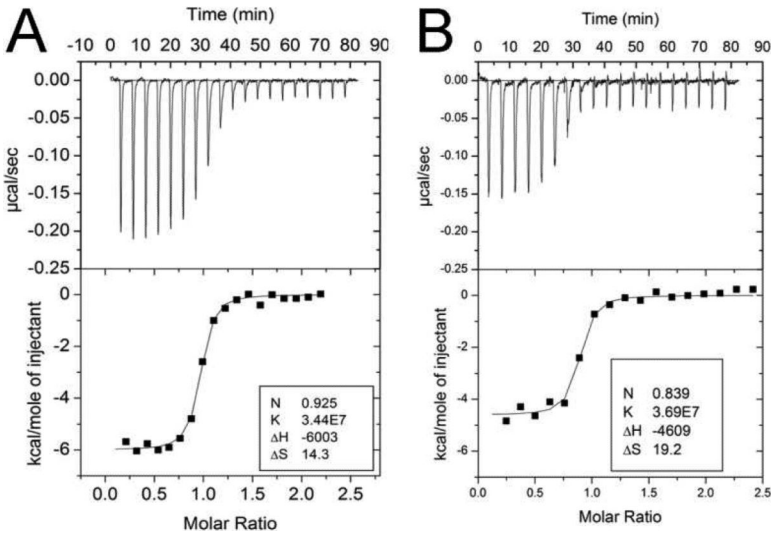

Figure 4.

ITC binding curves for 15 μL injections of a 70 μM solution of DAPA binding to thrombin alone (6.5 μM in the cell) (A) and to TM45-thrombin (6.5 μM thrombin with 32.5 μM TM45) (B).

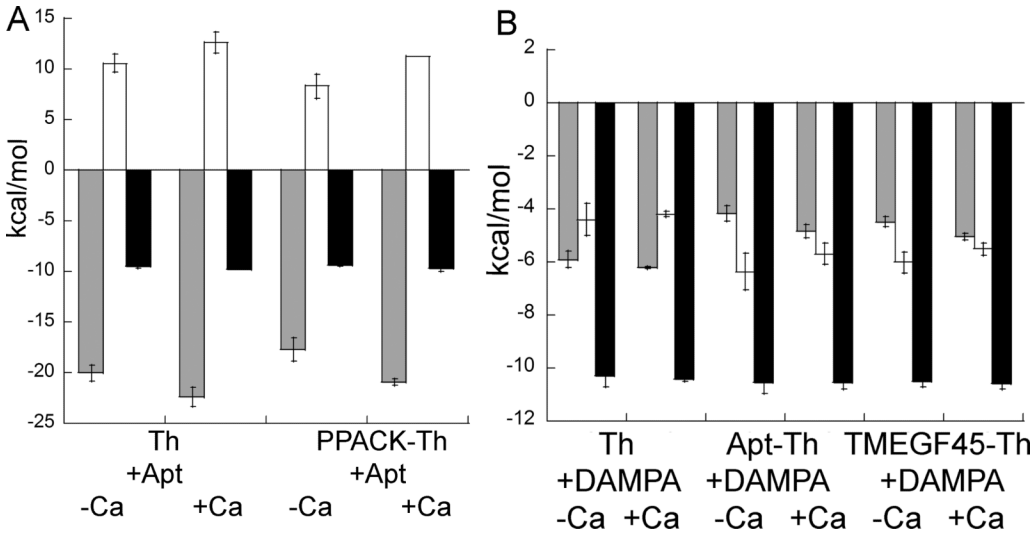

Figure 5.

(A) Thermodynamic parameters for Thrombin and PPACK-thrombin titrated with aptamer with and without Ca^{2+} present. (B) Thermodynamic parameters for aptamer-thrombin and TM45-thrombin with and without Ca^{2+} present. For both figures, ΔH is shown in gray, -TΔS is shown in blue, and ΔG is shown in dark red.

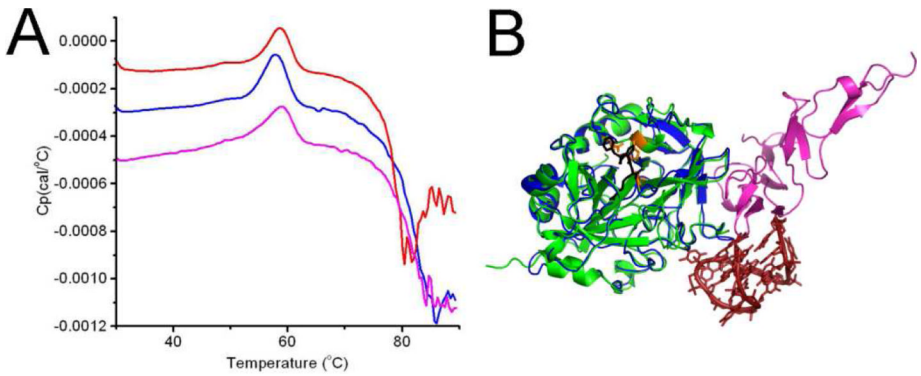

Figure 6.

(A) DSC thermal denaturation data for thrombin alone (25 μM, blue), aptamer-thrombin (25 μM thrombin with 75 μM aptamer, red), and TMEGF45-thrombin (25 μM thrombin with 100 μM TMEGF45, magenta). The denaturation temperatures are 57.9°C, 58.7°C, and 58.9°C respectively. (B) Overlay of the crystal structures of thrombin complexed with aptamer (thrombin - blue, aptamer - red) (PDB 1HUT (*34*)) and of thrombin complexed with TM456 (thrombin - green, TMEGF456 - magenta) (PDB 1DX5 (*14*)).

Table 1

Results from isothermal titration calorimetry experiments exploring binding at exosite1 and the active site of thrombin

Without calcium						
in cell	in syringe	K_a ($\times 10^7$ M^{-1})	N	ΔH (kcal/mol)	-TΔS (kcal/mol)	ΔG (kcal/mol)
thrombin	DAPA	4.5 ± 2.5[1]	0.9 ± 0.1	-5.9 ± 0.3	-4.4 ± 0.6	-10.3 ± 0.4
thrombin	aptamer	0.9 ± 0.2	0.96 ± 0.1	-20.2 ± 0.8	10.5 ± 0.9	-9.7 ± 0.2
thrombin	TM56	No heat observed				
apt-thromin	DAPA	5.8 ± 0.37	1.11 ± 0.1	-4.2 ± 0.3	-6.4 ± 0.7	-10.6 ± 0.4
ppack-thrombin	aptamer	0.8 ± 0.1	0.98 ± 0.02	-17.7 ± 1.1	8.3 ± 1.2	-9.4 ± 0.8
TM45-thrombin	DAPA	5.0 ± 1.8	0.86 ± 0.02	-4.5 ± 0.2	-6.0 ± 0.4	-10.5 ± 0.2

With 2.5 mM calcium						
thrombin	DAPA	4.5 ± 0.5	0.9 ± 0.1	-6.2 ± 0.04	-4.2 ± 0.1	-10.4 ± 0.1
thrombin	aptamer	1.5 ± 0.2	0.87 ± 0.04	-22.4 ± 0.1	12.6 ± 1.0	-9.8 ± 0.1
apt-thromin	DAPA	5.6 ± 2.1	1.06 ± 0.08	-4.8 ± 0.2	-5.7 ± 0.4	-10.5 ± 0.3
ppack-thrombin	aptamer	1.4 ± 0.6	0.9 ± 0.1	-21.0 ± 0.3	11.3 ± 0.004	-9.7 ± 0.3
TM45-thrombin	DAPA	5.9 ± 2.2	1.00 ± 0.06	-5.0 ± 0.1	-5.5 ± 0.2	-10.5 ± 0.2

[1] Values are the average of three independent experiments.